Chem. Mater. **2002,** *14,* 1314−1318

A Chiral Lead Borate Containing Infinite and Finite Chains Built up from BO_4 and BO_3 Units

Zhen-Tao Yu, Zhan Shi, Yu-Sheng Jiang, Hong-Ming Yuan, and Jie-Sheng Chen*

State Key Laboratory of Inorganic Synthesis and Preparative Chemistry,
Department of Chemistry, Jilin University, Changchun 130023, People's Republic of China

Received September 14, 2001. Revised Manuscript Received November 15, 2001

With a hydrothermal technique, a novel chiral lead borate ($Pb_6B_{11}O_{18}(OH)_9$) has been prepared. The sample has been characterized by powder X-ray diffraction, infrared spectroscopy, energy-dispersive spectroscopy, thermal analysis, and second-harmonic generation powder measurement. The structure of the compound, which crystallizes in the trigonal space group $P3_2$ with lattice constants $a = 11.7691(7)$ Å and $c = 13.3361(12)$ Å has been solved by single-crystal X-ray diffraction analysis. There exist infinite helical chains and finite chain fragments built up from BO_4 and BO_3 units. In the compound the Pb^{2+} cations are located in the space between adjacent polyborate anionic chains, compensating the negative charges of the chains. The chiral feature of the lead borate is unique, and because it lacks symmetry center, the compound exhibits distinct NLO properties.

Introduction

Non-centrosymmetric structure is a prerequisite[1,2] for a crystal to exhibit efficient bulk second-order nonlinear optical (NLO) effects that can be exploited in the manufacture of second-harmonic generator (SHG), electro-optical, and photorefractive devices.[3−5] A number of non-centrosymmetric compounds such as KH_2PO_4 (KDP), $KTiOPO_4$ (KTP), and $LiNbO_3$[6] have been found to be very useful as NLO materials and efforts have also been made to search for new NLO crystals during the past 2 decades. Because the polar orientation of inorganic triangular groups in crystals can lead to acentric structures and consequently favor NLO properties,[7] as evidenced by $K[B_5O_6(OH)_4]\cdot 2H_2O$ (KB_5),[8] β-$Ba_2B_2O_4$ (BBO),[9] LiB_3O_5 (LBO),[10] $Sr_2Be_2B_2O_7$ (SBBO),[11] and other borates containing triangular BO_3 units, more and more attention has been directed to crystalline borate compounds as potential NLO materials.[12−15] Nevertheless, it is worth pointing out that the NLO borate crystals were usually grown by a high-temperature flux method.

It has been demonstrated that hydrothermal and related techniques are very effective for the preparation of metastable crystalline materials such as zeolites and other compounds[16−21] that are capable of being used as catalysts, magnetic materials, and so on. Interesting non-centrosymmetric crystals such as $Na_4Ti_2Si_8O_{22}\cdot 4H_2O$,[22] $[(CH_3)_2NH_2]K_4[V_{10}O_{10}(H_2O)_2(OH)_4(PO_4)_7]\cdot 4H_2O$,[23] $[Co_4(2\text{-pzc})_4(V_6O_{17})]\cdot xH_2O$, and $[Ni_4(2\text{-pzc})_4(V_6O_{17})]\cdot xH_2O$[24] have also been obtained from hydrothermal systems. In an attempt to synthesize non-centrosymmetric compounds that are potentially applicable as NLO materials, we chose to grow lead borate crystals from hydrothermal reaction systems. The selection of lead borates for the investigation of structure−property relationships is of special interest because of the highly asymmetric bonding feature typical for a lead atom due to the stereoeffect of the $6s^2$ lone pair of Pb^{2+}. Little information about the structures of lead borates has appeared in the literature, and among the few lead borates are PbB_4O_7,[25] $Pb_6B_{10}O_{21}$,[26] $Pb_3B_{10}O_{18}\cdot 2H_2O$,[27] $Pb_2[B_5O_9]$-$(OH)\cdot H_2O$,[28] $Pb_5B_3O_8(OH)_3\cdot H_2O$,[29] $Pb[B_6O_{10}(OH)\cdot$

---

* To whom correspondence should be addressed: Fax: (+86) 431-567-1974. E-mail: chemcj@mail.jlu.edu.cn.

(1) Williams, D. J. *Angew. Chem., Int. Ed. Engl.* **1984**, *23*, 690.
(2) Zyss, J.; Oudar, J. L. *Phys. Rev. A* **1982**, *26*, 2028.
(3) Moerner, W. E.; Silence, S. M. *Chem. Rev.* **1994**, *94*, 127.
(4) Dalton, L. R.; Harper, A. W.; Ghosn, R.; Steier, W. H.; Ziari, M.; Fetterman, H.; Shi, Y.; Mustacich, R. V.; Jen, A. K.-Y.; Shea, K. J. *Chem. Mater.* **1995**, *7*, 1060.
(5) Dalton, L. R.; Harper, A. W.; Wu, B.; Ghosn, R.; Laquindanum, J.; Liang, Z.; Hubbel, A.; Xu, C. *Adv. Mater.* **1995**, *7*, 519.
(6) Dmitriev, V. G.; Gurzadyan, G. G.; Nikogosyan, D. N. *Handbook of Nonlinear Optical Crystals*; Springer-Verlag: Berlin, 1991.
(7) Xia, Y. *Adv. Mater.* **1994**, *6*, 510.
(8) Dewey, C. F., Jr.; Cook, W. R., Jr.; Hodgson, R. T.; Wynne, J. J. *Appl. Phys. Lett.* **1975**, *26*, 714.
(9) Chen, C. T.; Wu, B. C.; Jiang, A. D.; You, G. M. *Sci. Sinica* **1985**, *B28*, 235.
(10) Chen, C. T.; Wu, Y. C.; Jiang, A. D.; Wu, B. C.; You, G. M.; Li, R. K.; Lin, S. J. *J. Opt. Soc. Am.* **1989**, *6*, 616.
(11) Chen, C. T.; Wang, Y. B.; Wu, B. C.; Wu, K. C.; Zeng, W. L.; Yu, L. L. *Nature* **1995**, *373*, 322.
(12) Aka, G.; Kahn-Harari, A.; Vivien, D.; Benitez, J.-M.; Salin, F.; Godard, J. *Eur. J. Solid State Inorg. Chem.* **1996**, *33*, 727.
(13) Hu, Z. G.; Higashiyama, T.; Yoshimura, M.; Mori, Y.; Sasaki, T. *J. Cryst. Growth* **2000**, *212*, 368.
(14) Gruber, B. J.; Reynolds, T. A.; Keszler, D. A.; Zandi, B. *J. Appl. Phys.* **2000**, *87*, 7159.
(15) Wu, Y. C.; Liu, J. G.; Fu, P. Z.; Wang, J. X.; Zhou, H. Y.; Wang, G. F.; Chen, C. T. *Chem. Mater.* **2001**, *13*, 753.
(16) Williams, I. D.; Wu, M. M.; Sung, H. H−Y.; Zhang, X. X.; Yu, J. H. *Chem. Commun.* **1998**, 2463.
(17) Yamase, T.; Suzuki, M.; Ohtaka, K. *J. Chem. Soc., Dalton. Trans.* **1997**, 2463.
(18) Rijssenbeek, J. T.; Rose, L. J.; Haushalter, R. C.; Zubieta, J. *Angew. Chem., Int. Ed. Engl.* **1997**, *36*, 1008.
(19) Chen, J. S.; Thomas, J. M. *J. Chem. Soc., Chem. Commun.* **1994**, 603.
(20) Chen, J. S.; Pang, W. Q.; Xu, R. R. *Top. Catal.* **1999**, *9*, 93.
(21) Yuan, H. M.; Chen, J. S.; Shi, Z.; Chen, W.; Wang, Y.; Zhang, P.; Yu, J. H.; Xu, R. R. *J. Chem. Soc., Dalton. Trans.* **2000**, 1981.
(22) Roberts, M. A.; Sankar, G.; Thomas, J. M.; Jones, R. H.; Du, H.; Chen, J.; Pang, W.; Xu, R. *Nature* **1996**, *381*, 401;
(23) Soghomonian, V.; Chen, Q.; Haushalter, R. C.; Zubieta, J.; O'Connor, C. J. *Science* **1993**, *259*, 1596.
(24) Zheng, L. M.; Whitfield, T.; Wang, X.; Jacobson, A. J. *Angew. Chem., Int. Ed.* **2000**, *39*, 4528.

10.1021/cm010387k CCC: $22.00

Table 1. Crystal Data and Structure Refinement for $Pb_6B_{11}O_{18}(OH)_9$

empirical formula	$Pb_6B_{11}O_{18}(OH)_9$
formula weight	1803.12
temperature (K)	293(2)
wavelength (Å)	0.71073
crystal system	trigonal
space group	$P3_2$
unit cell dimensions	$a = 11.7691(7)$ Å $\alpha = 90°$
	$b = 11.7691(7)$ Å $\beta = 90°$
	$c = 13.3361(12)$ Å $\gamma = 120°$
volume (Å^3)	1599.7(2)
Z	3
ρ_{cal} (Mg/m^3)	5.615
absorption coeff. (mm^{-1})	47.325
F(000)	2316
crystal size (mm)	0.30 × 0.06 × 0.06
θ range for data collection	13.73−29.97°
limiting indices	$-16 \le h \le 16$, $-16 \le k \le 13$, $-18 \le l \le 17$
reflections collected	11078/5262
data/parameters	5262/398
goodness-of-fit on F^2	0.971
final R indices [$I > 2\sigma(I)$]	R1^a = 0.0681, wR2^b = 0.1170
largest diff. peak and hole	4.560 and −3.758 e Å^{-3}

[a] $R1 = \Sigma||F_o| - |F_c||/\Sigma|F_o|$. [b] $wR2 = [\Sigma[w(F_o^2 - F_c^2)^2]/\Sigma[w(F_o^2)^2]]^{1/2}$.

$B_2O(OH)_3]$,[30] and $Pb_6B_{12}O_{24}\cdot H_2O$.[31] Three of these compounds[25,28,29] exhibit NLO properties, but none have a chain feature. In this paper, we report the synthesis, X-ray crystal structure, and optical properties of a novel chiral compound, lead polyborate $Pb_6B_{11}O_{18}(OH)_9$ containing polyborate chains.

Experimental Section

Synthesis of Lead Polyborate $Pb_6B_{11}O_{18}(OH)_9$. The compound was synthesized by employing a hydrothermal technique. All reagents were of analytical grade. The reaction mixture of $Pb(CH_3COO)_2$ (1.90 g), H_3BO_3 (0.64 g), $H_2NCH_2CH_2NH_2$ (1.78 g), CH_3COOH (2.60 g), and H_2O (12.00 g) in a molar ratio of 1:2:7:7:133 was stirred until homogeneous, sealed in 20-mL Teflon-lined stainless steel vessels, and heated at 180 °C for about 2 days under autogenous pressure. The initial pH of the reaction system was ≈8.5. The resulting colorless columnar crystals were collected by filtration, washed with distilled water, and dried in air at ambient temperature without further separation.

General Characterization. The X-ray powder diffraction (XRD) patterns were recorded on a Siemens D5005 diffractometer using Cu Kα radiation ($\lambda = 1.5418$ Å) with a graphite monochromator. The recording speed was 8° min^{-1} over the 2θ range of 10−60° at room temperature. The IR spectra were collected on a Nicolet Impact 410 FTIR in the range of 400−4000 cm^{-1} using the KBr disk method. The differential thermal (DTA) and thermogravimetric analysis (TGA) were performed on a Perkin-Elmer DTA-1700 differential thermal analyzer and a Perkin-Elmer TGA-7 thermogravimetric analyzer, respectively, under a flow of dry air at a heating rate of 10 K min^{-1}. Energy-dispersive spectroscopy (EDS) was performed on a Hitachi EDAX DX-4 energy-dispersive analyzer.

Table 2. Atomic Coordinates (×10^4) and Equivalent Isotropic Displacement Parameters (Å^2 × 10^3) for $Pb_6B_{11}O_{18}(OH)_9$.

atom	x	y	z	U(eq)^a
Pb(1)	−2500(1)	9406(1)	1095(1)	13(1)
Pb(2)	−2744(1)	7909(1)	−3580(1)	13(1)
Pb(3)	3888(1)	9200(1)	364(1)	14(1)
Pb(4)	649(1)	5922(1)	1629(1)	14(1)
Pb(5)	7414(1)	5849(1)	83(1)	14(1)
Pb(6)	3927(1)	2778(1)	1357(1)	16(1)
B(1)	−2760(30)	8460(30)	−1120(20)	11(6)
B(2)	−720(30)	9930(30)	−2130(20)	4(5)
B(3)	−400(30)	9270(30)	−390(20)	10(5)
B(4)	1160(30)	8980(30)	800(20)	14(6)
B(5)	7930(30)	6090(30)	2430(20)	7(5)
B(6)	7290(30)	3750(30)	1718(19)	3(5)
B(7)	6630(30)	4020(30)	3440(20)	10(5)
B(8)	4540(30)	2240(30)	3960(20)	9(5)
B(9)	4890(30)	9390(30)	2550(20)	8(6)
B(10)	4100(30)	7120(30)	1770(20)	6(5)
B(11)	4450(30)	5560(30)	660(20)	11(6)
O(1)	−3734(17)	8842(18)	−707(13)	6(3)
O(2)	−3590(20)	7040(20)	−1383(16)	14(4)
O(3)	−2138(19)	9273(18)	−1981(13)	7(3)
O(4)	−1865(19)	8616(19)	−252(14)	10(4)
O(5)	−540(20)	9640(20)	−3209(15)	14(4)
O(6)	−60(20)	11430(20)	−2052(16)	13(4)
O(7)	−30(20)	9495(19)	−1445(14)	11(4)
O(8)	100(20)	8460(20)	51(15)	11(4)
O(9)	1721(19)	8290(19)	936(14)	9(4)
O(10)	9260(20)	7070(20)	2606(17)	20(4)
O(11)	7340(20)	6840(20)	1900(15)	12(4)
O(12)	7973(19)	5216(19)	1615(14)	9(4)
O(13)	7230(20)	5390(20)	3275(17)	19(4)
O(14)	6040(20)	3080(20)	1179(16)	17(4)
O(15)	8170(20)	3320(20)	1316(16)	15(4)
O(16)	7087(18)	3389(19)	2789(14)	8(3)
O(17)	5150(20)	3340(20)	3428(17)	19(5)
O(18)	3120(20)	1450(20)	3873(14)	12(4)
O(19)	6250(20)	10250(20)	2966(15)	13(4)
O(20)	3970(20)	8680(20)	3343(15)	14(4)
O(21)	4540(20)	10407(19)	2105(14)	11(4)
O(22)	4850(20)	8530(20)	1711(15)	13(4)
O(23)	2900(20)	6600(20)	1187(16)	17(4)
O(24)	3808(19)	6660(20)	2802(14)	12(4)
O(25)	4930(20)	6620(20)	1318(15)	11(4)
O(26)	5020(20)	4810(20)	578(17)	17(4)
O(27)	3310(20)	5250(20)	117(16)	14(4)

[a] U(eq) is defined as one-third of the trace of the orthogonalized U_{ij} tensor.

Second-Harmonic Generation Measurement. A powder second-harmonic generation test was carried out on the $Pb_6B_{11}O_{18}(OH)_9$ sample by means of the method of Kurtz and Perry.[32] Second-harmonic generation intensity data were obtained by placing a powder sample in an intense fundamental beam from a Q-switched Nd:YAG laser of wavelength 1064 nm. The output ($\lambda = 532$ nm), filtered first to remove the fundamental wavelength, was then detected using a photomultiplier and displayed on an oscilloscope. This procedure was then repeated using a standard NLO material, in this case microcrystalline KDP, and the ratio of the second-harmonic intensity outputs was calculated.

X-ray Diffraction Structural Analysis. A columnar crystal of lead polyborate $Pb_6B_{11}O_{18}(OH)_9$ with approximate dimensions 0.30 × 0.06 × 0.06 mm was selected and mounted on a Siemens SMART X-ray diffractometer with a CCD area detector. Data were collected using graphite-monochromatized Mo Kα radiation ($\lambda = 0.71073$ Å) at 293(2) K. The structure was solved by direct methods (SHELXTL Version 5.10) and refined by full-matrix least-squares on F^2 using SHELXTL Version 5.10 together with the absorption correction by an empirical method. All non-hydrogen atoms were refined anisotropically.

---

(25) Corker, D. L.; Glazer, A. M. *Acta Crystallogr. Sect. B* **1996**, *52*, 260.

(26) Krogh-Moe, J.; Wold-Hansen, P. S. *Acta Crystallogr. Sect. B* **1973**, *29*, 2242.

(27) Grube, H. H. *Fortschr. Mineral. Beih.* **1981**, *59*, 58.

(28) Belokoneva, E. L.; Dimitrova, O. V.; Korchemkina, T. A.; Stefanovich, S. Y. *Kristallografiya* **1998**, *43* (5), 864.

(29) Rastsvetaeva, R. K.; Arakcheeva, A. V.; Pushcharovsky, D. Y.; Vinogradova, S. A.; Dimitrova, O. V.; Stefanovich, S. Y. *Z. Kristallogr.* **1998**, *213* (4), 240.

(30) Belokoneva, E. L.; Korchemkina, T. A.; Dimitrova, O. V. *Russ. J. Inorg. Chem.* **1999**, *44*, 889.

(31) Belokoneva, E. L.; Dimitrova, O. V. *Russ. J. Inorg. Chem.* **1999**, *44*, 147.

(32) Kurtz, S. W.; Perry, T. T. *J. Appl. Phys.* **1968**, *39*, 3798.

Table 3. Selected Bond Lengths (Å) for $Pb_6B_{11}O_{18}(OH)_9$[a]

Pb(1)−O(4)	2.31(2)	Pb(4)−O(23)	2.43(2)
Pb(1)−O(7)#1	2.36(2)	Pb(4)−O(20)#6	2.54(2)
Pb(1)−O(18)#2	2.42(2)	Pb(4)−O(9)	2.59(2)
Pb(1)−O(1)	2.713(18)	Pb(5)−O(16)#7	2.369(19)
Pb(2)−O(18)#3	2.39(2)	Pb(5)−O(12)	2.378(19)
Pb(2)−O(5)	2.41(2)	Pb(5)−O(26)	2.53(2)
Pb(2)−O(3)	2.547(18)	Pb(5)−O(11)	2.71(2)
Pb(2)−O(20)#4	2.71(2)	Pb(5)−O(19)#8	2.73(2)
Pb(2)−O(6)#5	2.76(2)	Pb(6)−O(26)	2.32(2)
Pb(3)−O(9)	2.35(2)	Pb(6)−O(14)	2.34(2)
Pb(3)−O(22)	2.45(2)	Pb(6)−O(13)#7	2.51(2)
Pb(3)−O(24)#6	2.47(2)	Pb(6)−O(3)#9	2.665(19)
Pb(3)−O(21)	2.629(19)		
B(1)−O(3)	1.44(4)	B(6)−O(16)	1.47(3)
B(1)−O(2)	1.50(4)	B(6)−O(12)	1.51(3)
B(1)−O(4)	1.51(4)	B(7)−O(16)	1.41(4)
B(1)−O(1)	1.53(4)	B(7)−O(13)	1.43(4)
B(2)−O(3)	1.46(3)	B(7)−O(17)	1.51(4)
B(2)−O(7)	1.48(4)	B(7)−O(14)#10	1.52(4)
B(2)−O(5)	1.52(4)	B(8)−O(17)	1.33(4)
B(2)−O(6)	1.53(4)	B(8)−O(15)#10	1.39(4)
B(3)−O(7)	1.46(4)	B(8)−O(18)	1.46(4)
B(3)−O(5)#1	1.47(4)	B(9)−O(20)	1.45(4)
B(3)−O(8)	1.47(4)	B(9)−O(22)	1.49(4)
B(3)−O(4)	1.51(4)	B(9)−O(19)	1.51(4)
B(4)−O(9)	1.29(4)	B(9)−O(21)	1.57(4)
B(4)−O(6)#1	1.30(4)	B(10)−O(22)	1.45(4)
B(4)−O(8)	1.47(4)	B(10)−O(23)	1.45(4)
B(5)−O(13)	1.39(4)	B(10)−O(24)	1.45(4)
B(5)−O(10)	1.42(4)	B(10)−O(25)	1.50(4)
B(5)−O(12)	1.51(3)	B(11)−O(26)	1.35(4)
B(5)−O(11)	1.54(4)	B(11)−O(25)	1.39(4)
B(6)−O(15)	1.46(4)	B(11)−O(27)	1.40(4)
B(6)−O(14)	1.47(4)		

[a] Symmetry transformations used to generate equivalent atoms: (#1) $-x + y - 1, -x + 1, z + {}^1/_3$; (#2) $-y, x - y + 1, z - {}^1/_3$; (#3) $-x + y, -x + 1, z - {}^2/_3$; (#4) $-x + y - 1, -x + 1, z - {}^2/_3$; (#5) $-y + 1, x - y + 2, z - {}^1/_3$; (#6) $-y + 1, x - y + 1, z - {}^1/_3$; (#7) $-y + 1, x - y, z - {}^1/_3$; (#8) $-y + 2, x - y + 1, z - {}^1/_3$; (#9) $-x + y - 1, -x, z + {}^1/_3$; (#10) $-x + y + 1, -x + 1, z + {}^1/_3$; (#11) $-y + 1, x - y + 1, z + {}^2/_3$; (#12) $-x + y + 1, -x + 2, z + {}^1/_3$; (#13) $-x + y, -x + 1, z + {}^1/_3$; (#14) $-y + 1, x - y + 2, z + {}^2/_3$.

Of the 11078 reflections measured ($13.73° \le \theta \le 29.97°$), 5262 symmetry-independent reflections were used to solve the structure. On the basis of all these data and 398 refined parameters, $R1 = 0.0681$ [$I > 2\sigma(I)$], $wR2 = 0.1170$, and the goodness-of-fit on F^2 is 0.971. The highest peaks in the final difference map (4.560 e Å^{-3}) are near the Pb atoms. Relatively high residual electron densities are not unusual for Pb-containing compounds as observed previously.[33-35]

The experimental crystallographlic data for $Pb_6B_{11}O_{18}(OH)_9$ are listed in Table 1. The atomic coordinates with isotropic temperature factors are listed in Table 2, whereas the selected bond lengths are presented in Table 3.

Results and Discussion

Synthesis and General Characterization. The presence of ethylenediamine in the crystallization system seems to be critical for the growth of the crystals because, without ethylenediamine, no crystals of $Pb_6B_{11}O_{18}(OH)_9$ appear in the reaction product. The acetic acid is used to adjust the pH value of the reaction system.

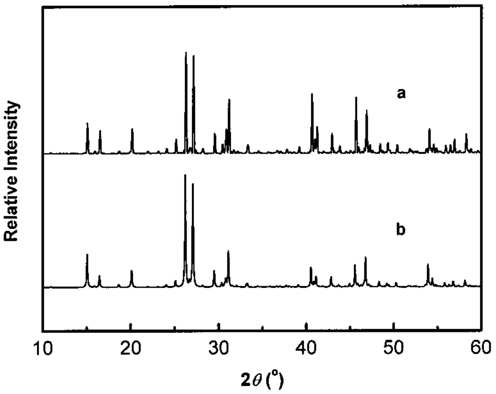

Figure 1. Powder X-ray diffraction patterns for $Pb_6B_{11}O_{18}(OH)_9$: (a) experimental and (b) simulated on the basis of the single-crystal structure.

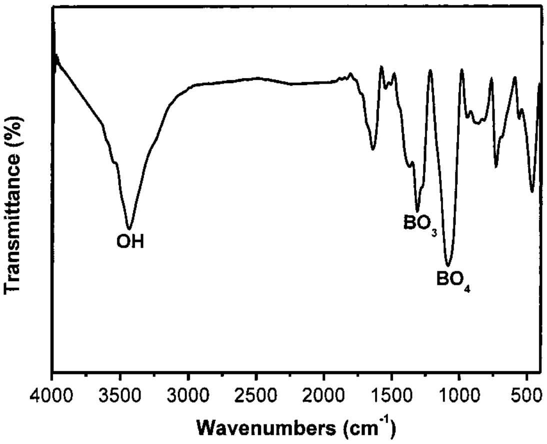

Figure 2. Infrared spectrum of $Pb_6B_{11}O_{18}(OH)_9$.

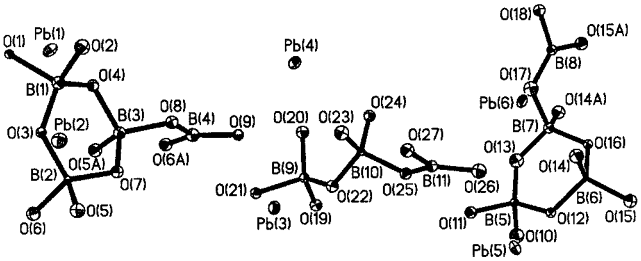

Figure 3. ORTEP drawing of the asymmetric unit of $Pb_6B_{11}O_{18}(OH)_9$. Thermal ellipsoids are shown at 50% probability.

Powder X-ray diffraction study of the crystals indicates that the product is phase-pure because the experimental XRD pattern corresponds well with the one simulated on the basis of the single-crystal structure (Figure 1). The intensity difference between the two patterns is believed to be caused by preferred orientation of the powder sample during collection of the experimental XRD data.

Energy-dispersive spectroscopy (EDS) shows the existence of Pb as a major component for the compound, and the infrared spectroscopy confirms the presence of triangular BO_3, tetrahedral BO_4, and OH groups in the structure (Figure 2). There exist two strong bands in the IR spectrum of the as-synthesized compound at about 1300 and 1080 cm^{-1}, respectively, in good agreement with the existence of BO_3 and BO_4 groups in the crystal structure. The band due to OH stretching vibrations is seen at around 3440 cm^{-1}.

Thermogravimetric analysis shows a weight loss of about 4.0% in the range from 100 to 750 °C in air,

---

(33) Norberg, S.; Svensson, G.; Albertsson, J. *Acta Crystallogr. Sect. C* **1999**, *55*, 356.

(34) Barbier, J.; Lévy, D. *Acta Crystallogr. Sect. C* **1998**, *54*, 2.

(35) Kubel, F.; Hagemann, H.; Bill, H. *J. Solid State Chem.* **2000**, *149*, 56.

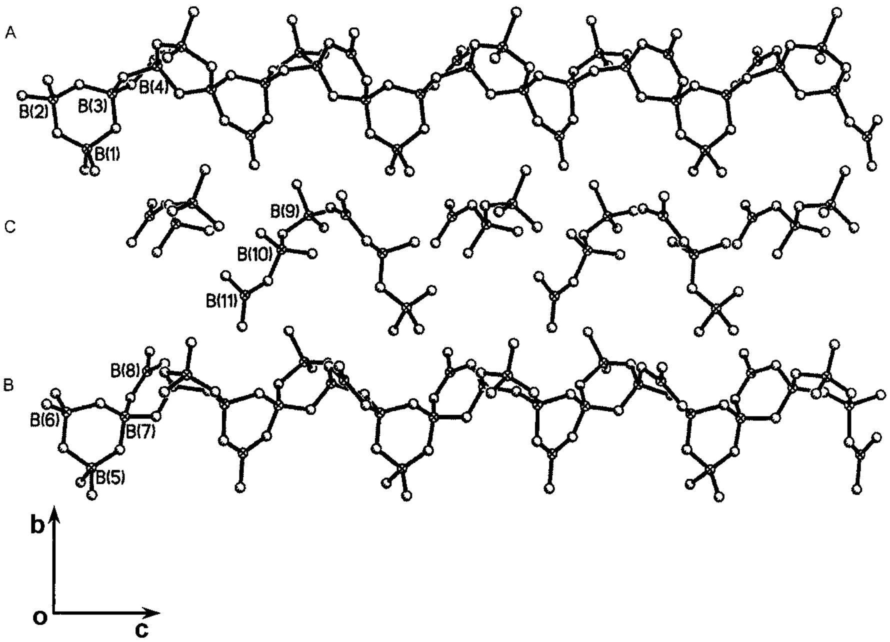

Figure 4. View of the chain structures along the *a* axis for $Pb_6B_{11}O_{18}(OH)_9$.

corresponding to the removal of the hydroxyl groups (calculated value 4.49%) that accompanies a distinct endothermic effect at around 410 °C as shown by the DTA curve. In addition, the crystals convert to glass form at about 600 °C.

Description of the Structure. The borate crystallizes in the trigonal space group $P3_2$. Furthermore, the unit cell is acentric, where optical activity can occur as specific physical effects.

The atom-labeling scheme of the compound is shown in Figure 3. The B−O bond lengths and O−B−O bond angles are in the range 1.29(4)−1.57(4) Å and 102(2)−127(2)°, which are in good agreement with those reported previously for other lead borates.

Single-crystal X-ray diffraction analysis reveals that the compound has a novel chiral structure consisting of three subunits, namely, infinite helical chains A and B with a composition of $[B_4O_8(OH)]_n^{5n-}$ and finite chain C of $B_3O_7(OH)_2^{7-}$ fragment (Figure 4). Chains A and B, both running along the *c* axis (Figure 5), are composed of nonplanar six-membered B_3O_3 rings which are found to join together by sharing the tetrahedrally coordinated B atoms. And in each B_3O_3 ring, the B and O atoms are strictly alternating, with the B atoms being bonded to three or four oxygen atoms. The central axis of each helical chain is a 3-fold screw axis. According to the hybrid orbital theory, the s and p orbitals of each three-coordinated B atom adopt sp^2 hybridization so that the three B−O bonds for the BO_3 units are nearly coplanar (B−O−B bond angles in the range 110(2)−125(3)°). In contrast, the s and p orbitals of a four-coordinated B atom take sp^3 hybridization, and as a result, the B atom resides in a distorted tetrahedral environment for the BO_4 units (B−O−B bond angles in the range 102(2)−116(2)°). The interconnection of the three- and four-coordinated B atoms through O bridges leads to a chain with a helical character. For chain C, three B atoms are linked into a finite chain through O bridges, which comprise a triangular BO_3 and two distorted tetrahedral BO_4 units. The average B−O distance for the BO_3 units (1.35 Å) in the infinite helical chain A is shorter than those in the infinite helical chain B (1.39 Å) and in the finite chain C (1.38 Å). For the triangular BO_3 groups the B−O bonds range from 1.29(4) to 1.47(4) Å, whereas the B−O distances for the BO_4 units in chains A, B, and C vary from 1.39(4) to 1.57(4) Å.

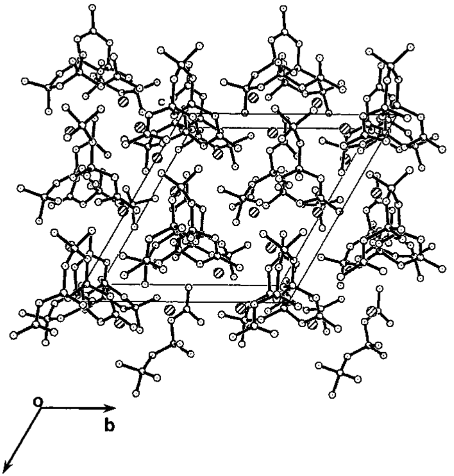

Figure 5. Structure for $Pb_6B_{11}O_{18}(OH)_9$ viewed along the *c* axis. Hashed circle, Pb; partly hashed circle, B; center-dotted circle, O.

Although a few chain borates such as $Na_3[B_5O_9]\cdot H_2O$,[36] LiB_3O_5,[37] LaB_3O_6,[38] and $Tl_2[B_4O_6(OH)_2]\cdot 2H_2O$[39]were discovered previously, none of them are chiral and no coexistence of infinite and finite chains was observed in these compounds.

The structure of our compound can be regarded as constructed from anionic borate chains, the negative

---

(36) Menchetti, S.; Sabelli, C.; Trosti-Ferroni, R. *Acta Crystallogr. Sect. B* **1982**, *38*, 2987.

(37) Wu, Y. C.; Jiang, A. D.; Lu, S. F.; Chen, C. T.; Shen, Y. S. *J. Synth. Cryst.* **1990**, *19*, 33.

(38) Abdullaev, G. K.; Mamedov, K. S.; Dzhafarov, G. G. *Kristallografiya* **1981**, *26*, 837.

(39) Touboul, M.; Bois, C.; Amoussou, D. *J. Solid State Chem.* **1983**, *48*, 412.

charges of which are compensated by the Pb^{2+} cations (Figure 5). The Pb^{2+} cations reside between adjacent chains of anions and they are believed to be responsible for holding the chain structures together mainly through electrostatic interactions with the chains. In this trigonal lead borate, there are three crystallographically different Pb atoms, coordinated to two types of oxygen atoms. One type is from a triangular BO_3 and the other from distorted tetrahedral BO_4 groups. The environment of Pb1, Pb3, and Pb6 consists of four O atoms in the range 2.31(2)−2.713(18) Å; that of Pb2 and Pb5 contains five O atoms in the range 2.39(2)−2.76(2) Å, whereas Pb4 is surrounded by three O atoms in the range 2.43(2)−2.59(2) Å. Furthermore, there is a bridging O atom between Pb3 and Pb4, and so is there between Pb5 and Pb6. On the whole, the Pb−O distances range from 2.31 (2) to 2.76(2) Å with an average value of 2.50(7) Å. These values are in accordance with those found in the literature where irregular coordination polyhedra about Pb atoms are often described.[25,29] In addition to the Pb^{2+} cations, nine protons must exist for each asymmetric unit of the compound to balance the negative charges on the chains. However, because none of the H atoms can be located through the structural analysis,[30] it is assumed that the H atoms are connected with 9 of the 13 terminal O atoms of the 3 types of chains in each asymmetric unit. Bond-valence analysis can be used to distinguish the O atoms and the OH groups. Among the 13 terminal oxygen atoms in the asymmetric unit, 4 (O9 of chain A, O18 of chain B, and O26 and O27 of chain C) are bound to trigonal planar boron centers. Three of the four planar B−O distances except for B8−O18 are significantly shorter than other terminal oxygen atoms (Tables 3). It is reasonable that these four terminal oxygens are solely oxo ligands. The relatively longer B8−O18 distance is probably due to the stronger interactions between O18 and Pb1 and Pb2 (Pb1−O18, 2.42(2) Å and Pb2−O18, 2.39 (2) Å). The remaining nine terminal oxygens (O1 and O2 of chain A; O10 and O11 of chain B; O19, O20, O21, O23, and O24 of chain C) in the BO_4 tetrahedra are assigned as hydroxo ligands. In addition, there are short O···O distances ranging from 2.333 to 2.996 Å between the terminal oxygens assigned as hydroxo ligands and the oxygens in adjacent chains. These short O···O distances between adjacent chains imply that H bonds, in addition to the Pb^{2+} cations, also play a role in holding the chains together.

NLO Properties. Second-order nonlinear optical effects for the powder sample of the compound have been investigated by optical second-harmonic generation (SHG) at room temperature. The investigation proves properties associated with the determined symmetry group, in particular, the lack of an inversion center. The intensity of the green light (frequency-doubled output: $\lambda = 532$ nm) produced by the trigonal lead borate $Pb_6B_{11}O_{18}(OH)_9$ crystal powder is about 1.2 times that produced by KDP powder, indicating that the trigonal $Pb_6B_{11}O_{18}(OH)_9$ has a powder SHG effect larger than that of KDP. The SHG signal provides a highly sensitive and definitive test of the absence of a center of symmetry for the compound.

Conclusions

When a hydrothermal technique is employed, a novel chiral lead borate compound is prepared, the structure of which contains infinite helical chains and finite chain fragments. The chiral feature of the compound is unique, and because it lacks symmetry center, the compound exhibits distinct NLO properties. The successful synthesis of the compound may help to explore new ways of synthesizing chiral materials that are potentially applicable in optical as well as other fields.

Acknowledgment. This work was supported by the National Natural Science Foundation of China and the Education Ministry of China.

Supporting Information Available: Tables of crystal data, structure solution and refinement, atomic coordinates, bond lengths and angles, and anisotropic thermal parameters for $Pb_6B_{11}O_{18}(OH)_9$ (PDF). This material is available free of charge via the Internet at http://pubs.acs.org.

CM010387K